Available online at www.sciencedirect.com
ScienceDirect
Vibrational Spectroscopy 43 (2007) 78–85
VIBRATIONAL SPECTROSCOPY
www.elsevier.com/locate/vibspec

Rejection criteria for open-path Fourier transform infrared spectrometry during continuous atmospheric monitoring

Limin Shao [a], Matthew J. Pollard [a,1], Peter R. Griffiths [a,*], Dale T. Westermann [b], David L. Bjorneberg [b]

[a] *Department of Chemistry, University of Idaho Moscow, ID 83844-2343, USA*
[b] *USDA-ARS, NW Irrigation & Soils Research Laboratory, 3793 N 3600 E, Kimberly, ID 83341, USA*

Received 27 April 2006; received in revised form 24 June 2006; accepted 26 June 2006
Available online 17 August 2006

Abstract

Over 32,000 interferograms measured during open-path Fourier transform infrared (OP/FT-IR) measurements at dairy and hog farms were evaluated for anomalies. Five types of anomalies could be distinguished: a reduction in the interferogram intensity because of weather-related optical misalignment; an increase in the amplitude of interferograms measured with too short a path-length that leads to a non-linear detector response; a periodic interference caused by wind-induced vibrations; the presence of spikes in the interferogram; and an increase in the noise level of the interferogram (and hence of the spectrum) because of the effect of electrical interference. Prior to testing for the presence of anomalous data, each interferogram is subjected to a high-pass filter. A noise level index is then calculated from the wings of the interferogram and interferograms are rejected if the value of this parameter is too high. When the criteria developed in this project are applied, OP/FT-IR spectra may be measured at 1-min intervals over a period of several days.

Keywords: Open-path; Atmospheric monitoring; FT-IR; Interferogram rejection

1. Introduction

With typical detection limits of ~10 ppb for most volatile compounds [1], open-path Fourier transform infrared (OP/FT-IR) spectrometry is a sensitive, non-invasive technique for atmospheric monitoring. Analytes include hazardous air pollutants [2], airborne toxic industrial chemicals [3], and greenhouse gases [4]. The task of continuous, automated monitoring at high temporal resolution and over fairly long periods of time by OP/FT-IR spectrometry has been facilitated by the development of fast personal computers with large storage capacity.

In principle, OP/FT-IR measurements can be made continuously over periods of several hours or even days at intervals of ~1 min. There are certain practical drawbacks to this technique, however. OP/FT-IR measurements may be affected by uncontrolled or unpredicted ambient factors such as wind, rain, snow, and dust; for example, wind can cause the optics to become misaligned and may enhance the concentration of airborne dust, while rain and snow attenuate the beam and increase the water content of the atmosphere, potentially decreasing the usable OP/FT-IR windows. Furthermore, the infrared beam may occasionally be interrupted by traffic or birds that completely or partially block the beam. Even though quality control (QC) or quality assurance (QA) procedures have been developed for OP/FT-IR spectrometry [5–7] these procedures may be quite difficult to implement when the instrumentation is unattended for extended periods of time. Depending on how the interferograms are affected, some may still contain useful analytical information, while others must be rejected or else they may potentially yield erroneous concentrations for the target molecules. In this paper, we distinguish between several categories of interference in OP/FT-IR spectrometry and propose ways in which those anomalous interferograms that contain useful data are retained while the others are rejected.

Several important issues for QC or QA protocols during continuous OP/FT-IR spectrometry can be cited. Firstly, the amount of data generated is large; continuous monitoring with interferograms measured once every ~70 s (the condition under

* Corresponding author. Tel.: +1 208 885 5807; fax: +1 208 885 6173.
E-mail address: pgriff@uidaho.edu (P.R. Griffiths).
[1] Present address: Department of Chemistry, Washington State University, Pullman, WA 99164-4630, USA.

0924-2031/$ – see front matter © 2006 Published by Elsevier B.V.
doi:10.1016/j.vibspec.2006.06.016

which we run our instrument) generates over 1000 interferograms per day, or ~250 Mbytes in spc format (Thermo Galactic, Madison, WI). When the meteorological or environmental conditions are poor (high winds, dust, rain, snow, or fog), the percentage of invalid interferograms may be larger than 10%. Thus sometimes over 100 interferograms per day may have to be recognized as invalid and rejected when the measurements are made under conditions of inclement weather. Secondly, the ambient factors mentioned above could affect the true path-integrated concentration of the target molecules; for example a high wind could rapidly remove pollutants from the infrared beam. Thus simply rejecting an anomalous result because it appears to be out-of-line with the predicted concentrations determined immediately beforehand could lead to important atmospheric changes being missed. Thirdly, even for invalid measurements, the quantitative method could result in apparently normal, but nonetheless incorrect, concentrations being calculated. Thus distinguishing between "good" and "bad" results based solely on whether the predicted concentrations "appear" to be logical is, therefore, fraught with risk.

We have made a detailed investigation of over 32,000 OP/FT-IR interferograms measured in and around dairy and hog farms in Southern Idaho, USA, in conditions that ranged from calm, summer weather to cold, snowy, windy winter weather and we report the results in this paper. We found that interferences could be classified into five types based on how the interferogram or the resulting single-beam spectrum had been affected. From this study, an automatic exclusion procedure was developed to identify those interferograms that should be rejected. Our results have shown that most invalid OP/FT-IR interferograms could be identified and prevented from entering further process steps, even though the inteferogram may provide analytical data that appear to be correct. As a result of this process, data analysis of OP/FT-IR measurements and the interpretation of these results have been effectively and efficiently improved. After exclusion of the false results, the burden on the practical QC or QA is lessened considerably.

2. Experimental

OP/FT-IR measurements were carried out in June and July 2004, and January, March, and June 2005 on and around a dairy farm in southern Idaho in a cooperative project for monitoring gaseous emissions with the Northwest Irrigation and Soil Research Laboratory (NWISL) of the United States Department of Agriculture (USDA). The OP/FT-IR spectrometer was manufactured by MDA Corporation (Atlanta, GA), and incorporated a Bomem Michelson 100 interferometer, a 31.5-cm telescope, a cube-corner array retroreflector and a Sterling-engine-cooled mercury cadmium telluride (MCT) detector. Instrument control and data acquisition were done with GRAMS 7.00 (Thermo Galactic, Salem, NH). The distance between the telescope and retroreflector usually ranged between 50 and 150 m, but occasionally longer path-lengths were necessary. Every OP/FT-IR interferogram was measured at a nominal resolution of 1 cm^{-1} by co-adding 16 interferograms. For simplicity, only those interferograms measured in the "forward" direction were co-added; interferograms generated in the "reverse" direction were discarded. The data acquisition frequency, i.e., the frequency of the HeNe laser reference interferogram, was 20 kHz. All spectra for the analysis were computed with a zero-filling factor of 8 and Norton–Beer "medium" apodization. These measurement conditions were found to give an acceptable tradeoff between the signal-to-noise ratio (SNR) and time resolution for continuous monitoring.

The transmittance at wavenumber $\tilde{\nu}$, cm^{-1}, $T(\tilde{\nu})$, was measured by calculating the ratio of a long-path spectrum to a short-path background spectrum measured with the retro-reflector located one or two meters from the telescope and converting to absorbance, $A(\tilde{\nu})$, i.e., $-\log_{10}T(\tilde{\nu})$. For the short-path background spectrum, a metallic screen was placed over the entrance aperture of the telescope to attenuate the signal so that the response of the MCT detector varied linearly with the intensity of the interferogram. Absorbance spectra measured in this way showed many strong lines from the vibration–rotation spectrum of water and often had less than perfect baselines. Even so, provided that the variation in the intensity of the water lines, the air temperature and the baselines of the spectra in the calibration set covered the range of the these parameters in spectra measured in the field, good analytical data could be obtained by the partial least squares (PLS) regression technique described below.

The most commonly used algorithm to obtain quantitative data from OP/FT-IR spectra is classical least squares regression (CLS). However, for CLS to be applied accurately, only the information from one molecule should contribute to the spectrum in the region of interest [5]. Previous workers have developed a variety of ways to compensate for atmospheric water vapor lines in the spectrum so that they do not interfere with the absorption spectrum of the analyte(s) [5–7]. Unfortunately, none of these approaches is readily implemented to give automated removal of water lines from the spectrum and we have found that CLS regression is inappropriate for automated OP/FT-IR spectra measured under anything other than calm, clear conditions. We have shown that PLS regression overcomes many of the drawbacks of CLS for OP/FT-IR spectrometry [8]. Calibration spectra are synthesized by measuring single-beam OP/FT-IR spectra in a pristine environment (i.e., where no analytes other than atmospheric H_2O, CO_2, CH_4, and N_2O are present in the infrared beam). These spectra are measured over different path-lengths, at different temperatures and relative humidities so that they represent the full range of conditions under which subsequent OP/FT-IR spectra are expected to be measured. Each long-path spectrum is then ratioed against a short-path single-beam spectrum of the type described in the previous paragraph and converted to absorbance. Reference spectra of each analyte are randomly scaled and added to the absorbance spectrum of the background and used as the calibration set for PLS regression.

Many factors contribute to the variance of the background, including the path-integrated concentration of atmospheric H_2O and CO_2, the fact that all strong lines in the vibration–rotation spectrum vary with the path-integrated concentration of the analytes in non-linear fashion, the effect of temperature

on these lines and the effect of a poor baseline. These factors were accounted for by including at least nine eigenvectors in the PLS regression to account for variance in the background and one additional eigenvector for each analyte in the spectral region being investigated in the way that was reported by Hart and Griffiths [9] Quantitative determinations of ammonia and methane were performed by PLS regression of the spectral data from 1250 to 750 and 3200 to 2850 cm^{-1}, respectively.

3. Results and discussions

A typical open-path interferogram and the corresponding single-beam spectrum measured under stable conditions are shown in Fig. 1. The appearance of many OP/FT-IR interferograms measured under unstable conditions was found to be visibly different from the one shown in Fig. 1a. By visual inspection, the anomalous interferograms could be classified into the following five types.

3.1. Low centerburst intensity

In the simplest class of anomalous interferograms, the intensity of the centerburst (at zero path difference), was sometimes observed to vary significantly, especially under windy conditions. This variation is caused by misalignment of the telescope so that the beam partially missed the retroreflector. Even though a low centerburst intensity leads to a reduction in the amplitude of the calculated single-beam spectrum, a reduced SNR does not necessarily result in an invalid measurement when concentrations are calculated by our PLS technique. However, when the centerburst intensity is excessively low, the SNR was found to be inadequate for a meaningful result to be obtained. In our investigation, when the retroreflector and telescope were correctly aligned, the maximum value of the interferogram at the centerburst was approximately 4 V (see Fig. 1a). (The maximum signal that could be input to the analog-to-digital converter (ADC) was 5.6 V.) When the centerburst intensity fell below 1 V, the signal-to-noise ratio of the spectrum was too low to allow the concentration of ammonia or methane to be predicted accurately by our PLS regression technique, in part because of the low SNR and in part because no spectrum with a baseline above 0.6 absorbance units was included in the calibration set. Thus for the particular instrument and the quantitative method used, any time that the centerburst intensity fell below 1 V, the interferogram was rejected. Usually this condition was encountered when the signal dropped below 25% of its value when the system was well aligned.

3.2. High centerburst intensity

Another extreme case occurs when the intensity at the centerburst is too high. This circumstance was usually found when the distance between the detector and the retroreflector was below 50 m. Once the instrument was setup in the field and aligned properly, the gain on the detector's amplifier was maximized to yield a centerburst signal of between 4.0 and 4.5 V. On windy days, when it was difficult to align the optics perfectly, the effect of wind could actually improve the alignment slightly. If the centerburst intensity is too high, the non-linear response of the MCT detector leads to a photometric error [10]. Under conditions of very high photon flux, the dynamic range of the ADC can be exceeded, which leads to an even greater photometric error [11]. As noted above, when the short path-length background spectrum was measured, a metallic screen was attached to the front of the telescope to attenuate the beam. However, even with the screen installed the centerburst intensity could sometimes be too high. To avoid this situation in our investigation, any interferogram in which the maximum data point exceeded 5.2 V was rejected.

3.3. Low-frequency interference

Occasionally, some interferograms were visually observed to contain extraneous low-frequency components, as shown by Fig. 2a1 and a2. Fourier transforms of the two interferograms in Fig. 2 were calculated to determine the frequency of these components, and the results are shown as Fig. 2b1 and b2. In the spectra computed from these two interferograms, large spikes were observed at ~8 and ~25 cm^{-1}, respectively.

In most FT-IR spectrometers, including the one that we used, the infrared interferograms are sampled at every second zero-crossing of the interferogram of a helium–neon laser. If the data acquisition frequency is f_{HeNe}, Hz, an interfering sine wave of frequency f gives rise to a spike in the spectrum at a wavenumber given by:

$$\tilde{\nu} = \frac{15,800\, f}{f_{HeNe}} \text{ Hz} \quad (1)$$

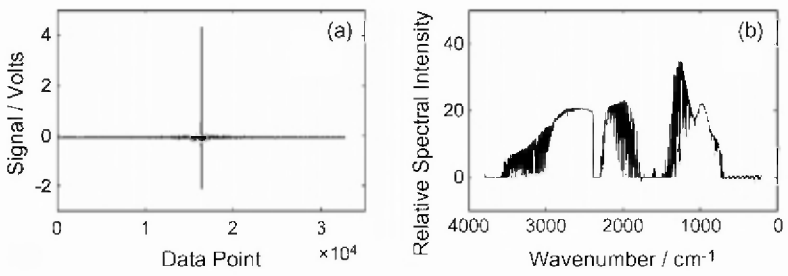

Fig. 1. (a) A normal OP/FT-IR interferogram and (b) the corresponding single beam spectrum. The distance between the instrument and the retroreflector was 159 m to yield a total path-length of 318 m.

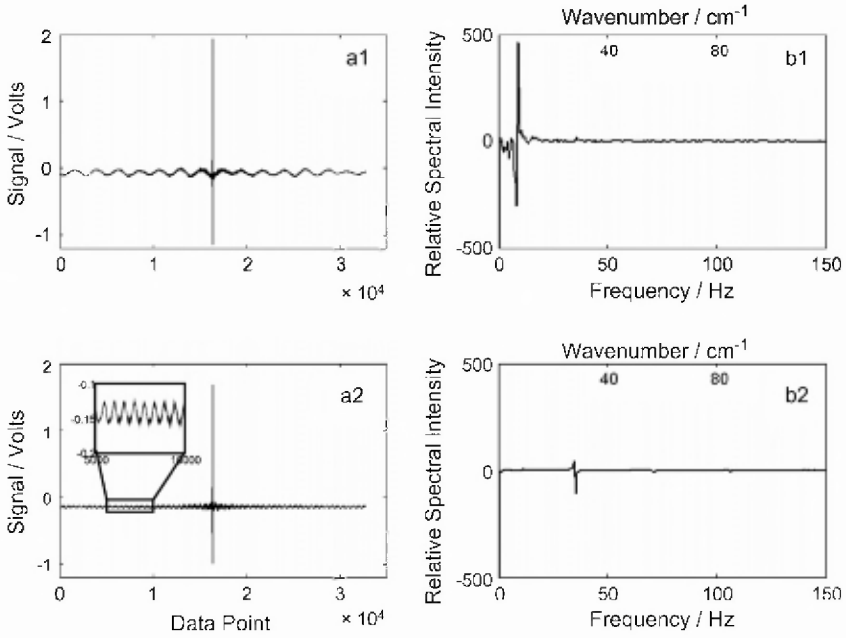

Fig. 2. Interferograms (a1 and a2) with extrinsic low-frequency components and their corresponding Fourier transformed signals (b1 and b2). The amplitude of the spike at 10 Hz in (b1) is over ten times greater than the peak amplitude of the spectrum in Fig. 1b.

where 15,800 cm^{-1} is the wavenumber of the HeNe laser. Since $f_{HeNe} = 20{,}000$ Hz for our system, $\tilde{\nu} = 0.79 f_v$ Hz or $f_v = 1.266\tilde{\nu}$. Thus the frequencies of the sinusoidal waves in Fig. 2a1 and a2 are ~10 and ~32 Hz, respectively.

The cut-on wavenumber for the MCT used in our work was about 700 cm^{-1}. In practice, therefore, even though the affected interferograms look rather ugly, the presence of any spike in the single-beam spectrum below 500 cm^{-1} does not have a deleterious effect on the absorbance spectrum between 700 and 4000 cm^{-1} in which all the analytical absorption bands are located.

To determine the cause of the sinusoidal interference, we first made an estimate of its amplitude by calculating the standard deviation of the first quarter of the data points in the interferogram located prior to the centerburst. This region contains information from the sharp vibration–rotation lines of atmospheric water vapor as well as the detector noise. For well-aligned interferograms such as the one shown in Fig. 1a, the standard deviation usually varies between about 0.004 and 0.01 V. When there was a low-frequency sinusoidal interference, the value of the standard deviation could be as high as 0.1.

Interference of this type is caused by the vibration of one or more of the optical components [12]. To investigate whether the effect of wind was to cause one of the components to vibrate, 373 interferograms were measured continuously from 13:48 to 20:54 on March 17, 2005 over the feedlot of a dairy farm. For each interferogram, a standard deviation was calculated over the first quarter of points, and used to estimate the amplitude of the low-frequency vibration. All interferograms were visually inspected to exclude any other factors that might have contributed to a change in the standard deviation.

The connection between the standard deviation and wind speed is shown by the data in Fig. 3. When the wind speed was less than ~4 m s^{-1}, no obvious low-frequency components could be observed in the corresponding interferograms and the standard deviation was ~0.01 V. Only when the wind speed exceeded 4 m s^{-1} were these fluctuations observed. A similar correlation was observed from several other monitoring sessions in which wind speed fluctuated considerably. For all OP/FT-IR measurements, the instrument and the retroreflector were mounted on tripods that were anchored to the ground. Although all components are sturdy, the telescope and retroreflector are large and can vibrate when the wind speed exceeds a certain level, causing low-frequency sinusoidal intensity variations of the reflected infrared beam.

For reasons that will become apparent in the next section of this paper, the effect of this type of interference was removed by applying a high-pass filter to the interferogram in the following way. After computing the single-beam spectrum from the measured interferogram, all values in the spectrum below

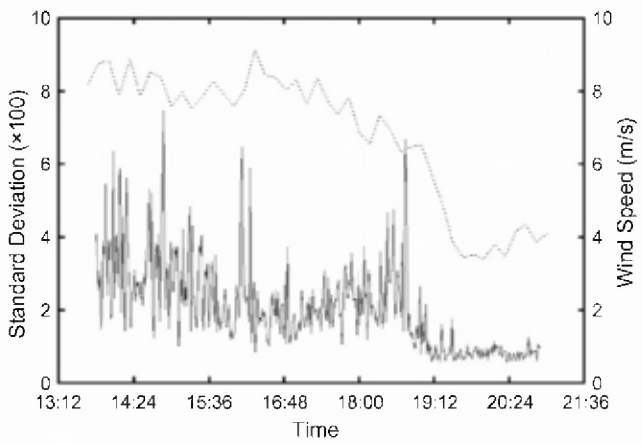

Fig. 3. The standard deviations of the first or last 25% of the points of the interferograms in a continuous monitoring session. The broken line shows the wind speed at the time of the measurement.

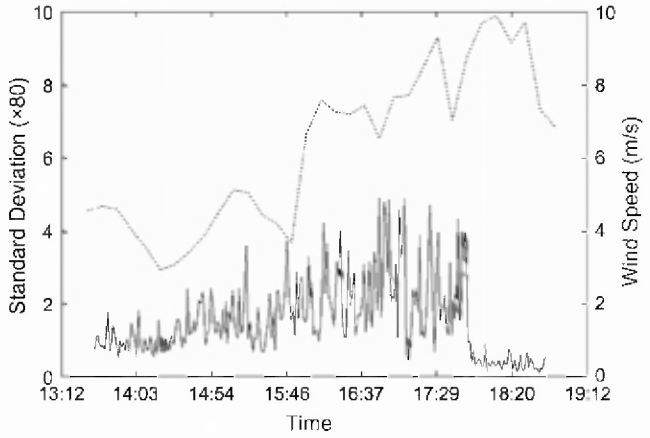

Fig. 4. The standard deviations of the first or last 25% of the points of the interferograms in a continuous monitoring session. The broken line shows the wind speed variation. The instrument lost alignment at about 17:50.

500 cm^{-1} were set to zero. The inverse Fourier transform was then calculated in order to recover the interferogram with all frequency components below 633 Hz (1.266 × 500, Eq. (1)) removed. As noted above, the low-frequency interference does not affect the quantitative accuracy of OP/FT-IR measurements. Indeed, in the above instance, all 373 interferograms produced valid absorbance spectra for the analysis.

Sometimes strong winds lead to a more severe problem than introducing a vibration in one or more of the optical components. The results obtained when the atmosphere over the same feedlot was monitored from 13:35 to 18:44 on March 16, 2005 are shown in Fig. 4. The standard deviation of the wings of each interferograms was calculated in the same way used to obtain the data in Fig. 3. Visual inspection of the interferograms showed that the low-frequency components appeared about 1 h after the beginning of data acquisition. After 16:10, when the wind speed was higher than 7 m s^{-1}, most of the interferograms were found to exhibit the low-frequency interference. After 17:50, when the wind speed exceeded 9 m s^{-1}, the centerburst intensity of all interferograms dropped below 0.2 V, which is the signal from internal reflections inside the sealed instrument. Under these conditions, the wind had misaligned the infrared beam to the point that the signal at the detector was too small for the effect of vibrations to be observed. Thus interferograms measured after 17:50 were invalid based on the intensity of the centerburst, and the rest yielded acceptable results even with the severe low-frequency interference.

3.4. High-frequency noise

Occasionally, the noise level of the interferograms was found to increase dramatically even though the noise level of neighboring interferograms was normal. An example of this effect is shown in Fig. 5a1 and b1. The first interferogram and spectrum in this time series (measured 25 min earlier) are shown in Fig. 5a2 and b2, respectively. Note that the centerbursts of these two interferograms have approximately the same value, so the poor SNR of the spectrum shown in Fig. 5b1 is a result of increased noise, not decreased signal. The amplitude of the high-frequency noise in the interferogram does not vary with the optical path difference. This characteristic makes it possible to distinguish noisy interferograms from normal ones.

Whereas the low-frequency interference described in the previous section can be removed using a high-pass filter, the high-frequency noise seen in the interferogram in Fig. 5a1 cannot be removed without a loss of spectral information. Thus interferograms with excessive high-frequency noise should be rejected with minimal further data processing. Considering the large number of interferograms acquired during continuous monitoring, any algorithm used to reject noisy interferograms

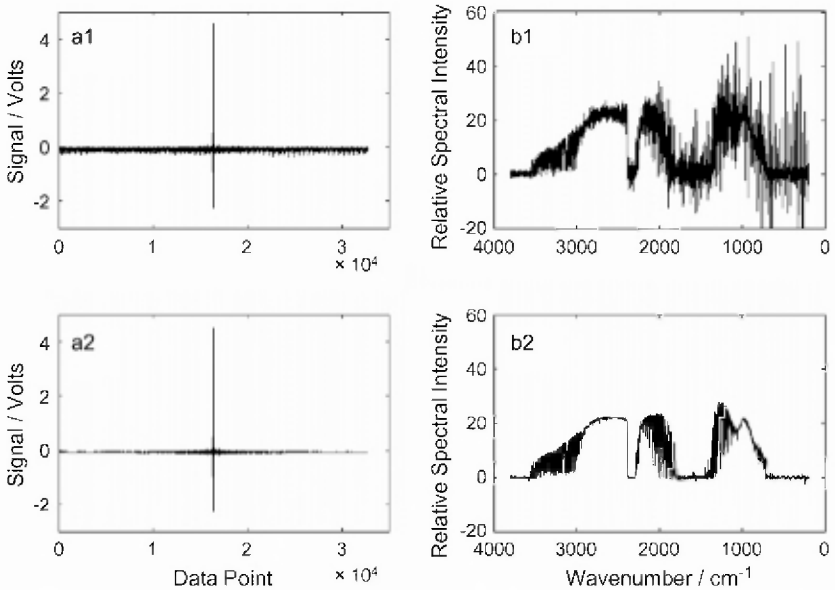

Fig. 5. An interferogram (a1) with high-frequency noise from a monitoring session. The interferogram shown in (a2) is the first one of the session. Corresponding single-beam spectra are shown in plot (b).

needs to be reliable, fast, and automatic. Let the subscripts i and 1 refer to the ith and the first interferogram from one continuous set of measurements. To develop criteria for which "bad" interferograms can be rejected, three reasonable assumptions are made: (a) the first interferogram of a set is always measured immediately after the system has been aligned and is, therefore, deemed to be normal; (b) the signal is proportional to the maximum value of the interferogram, H_i; and (c) the noise may be estimated by calculating the standard deviation of the data over the first quarter of points in the interferogram before the centerburst or the last quarter of the points after the centerburst, $STD_{1/4}$. Obviously these points also contain real spectral information but for OP/FT-IR spectrometry at $1\ cm^{-1}$ resolution the noise level of "bad" scans exceeds the signal, as can be seen in Fig. 5a1.

To recognize such bad scans, a *noise level index* for the ith interferogram (NLI_i) is calculated as

$$NLI_i = \frac{STD_{1/4,i}H_1}{STD_{1/4,1}H_i} \quad (2)$$

Interferograms are rejected if NLI_i is significantly greater than 1; for our work, an interferogram is rejected if $NLI_i > 1.3$.

This procedure would be adequate if interferograms never exhibited the low-frequency interference discussed in the previous section. As noted above, however, the presence of a low-frequency sinusoidal interference does not mean the interferogram must be rejected, provided that the interfering frequency is less than 633 Hz. In order that interferograms showing a low-frequency interference are not rejected simply because $NLI_i > 1.3$, every interferogram is subjected to the high-pass filtering procedure described in the previous section prior to calculating the noise level index.

For the monitoring session mentioned above, we checked all the 520 interferograms and found that less than 5 min after the measurement of the interferogram shown in Fig. 5a1, the interferograms were normal again. We also checked the meteorological data, such as wind speed and temperature, at that time, and no anomaly was found. Thus the sudden appearance of high-frequency noise must be caused by electrical interference from the generator that was used to supply the electrical power in the field.

3.5. Spikes

On some occasions, spikes were found in our OP/FT-IR interferograms. These spikes could be broad or narrow, as shown in Fig. 6a1 and a2. The broad spike is caused by an object (e.g., a bird) passing through the infrared beam. For the spike in Fig. 6a1, the duration of the spike was found to be 0.04 s. The diameter of the mirror of the telescope of our OP/FT-IR spectrometer is 31.5 cm. In this case, the speed of the moving object is calculated to be $28\ km\ h^{-1}$, about the normal speed of either a bird or a vehicle. The same explanation cannot be given for the narrow spikes in Fig. 6a2. The average duration of the spike is about 0.006 s; thus an object would need to travel at a speed of $189\ km\ h^{-1}$, which is extremely unlikely. It is much more probable that narrow spikes and noise of the type seen in Fig. 6a2 are caused by unstable electronics that, caused the increased noise level discussed in the previous section.

One bad point in the interferogram would cause a sinusoidal oscillation across the entire the spectrum. The further the distance of the spike from the centerburst, the higher is the frequency of the oscillation. Fig. 6b2 shows how the single-beam spectrum is affected. We found that PLS regression yielded erroneous results any time that the amplitude of a narrow spike in the interferogram is excessively high. Interferograms with this problem must be rejected.

As the width of the spike increases, the sinusoidal oscillation decays with increasing wavenumber. If the spike is broad

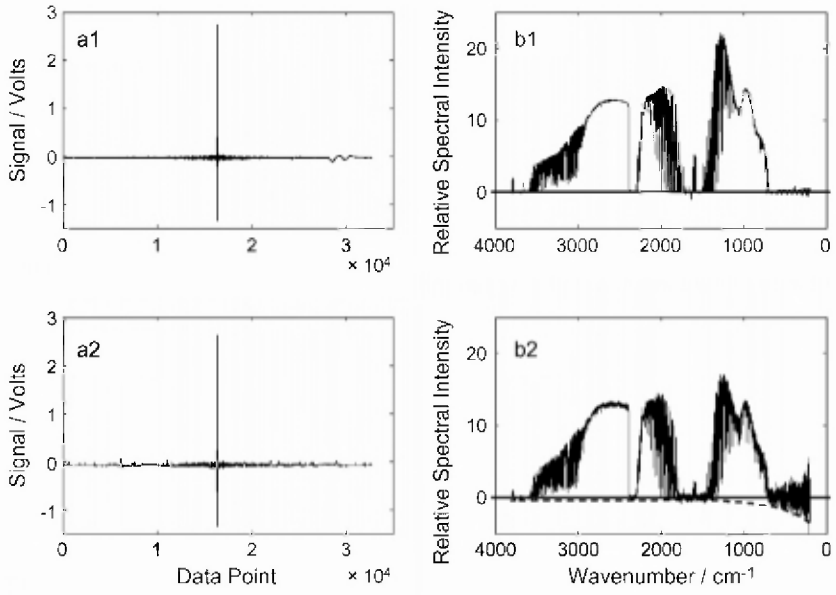

Fig. 6. Interferograms with broad (a1) and sharp (a2) spikes, and their corresponding single-beam spectra (b1 and b2). The horizontal lines in (b1 and b2) mark the zero line. The broken line in (b2) is the estimated profile of the decay.

enough that the oscillation in the spectrum has decayed sufficiently as the wavenumber increases from zero to 700 cm^{-1}, the effect of the spike on the accuracy of the determination of the target molecules is negligible. This is the case for the data shown in Fig. 6a1 and b.1. Whereas the noise below the detector cut-off ($\tilde{\nu} < 700\,cm^{-1}$) is too high to allow acceptable quantification, the noise above the cut-off in the single-beam spectrum is low enough to be acceptable, i.e., reasonable values for the concentration of ammonia and methane were obtained by PLS regression.

It should be noted that the amplitude of the oscillation is also controlled by the magnitude of the spike. Small, broad spikes do not create a severe problem, whereas this is not the case for narrow spikes. The effect of broad spikes (even ones as large as the one shown in Fig. 6a1) can be largely be removed by the action of a high-pass filter, as the filtered interferogram gives a normal NLI_i value. On the other hand, for an interferogram containing a narrow spike of any amplitude, or intense broad spike, the calculated NLI_i value is too high to permit adequate quantification. For the two interferograms in Fig. 6, the NLI_i values calculated after high-pass filtering were found to be 1.4 (narrow spikes) and 1.1 (broad spikes).

4. Conclusions

From the inspection of over 32,000 interferograms measured during OP/FT-IR spectrometry, five causes of error were observed.

- A reduction in the interferogram intensity because of weather-related optical misalignment can reduce the signal to an unacceptably low value. Any time the highest point in the interferogram falls below a predetermined value, the noise in the spectra is too high to allow acceptable quantification and the interferogram is rejected; in our measurements when the distance between the telescope and retroreflector was 120 m or less, this value was 25% of the initial value.
- An increase in the amplitude of interferograms measured with too short a path-length can lead to a non-linear response of the MCT detector and hence poor photometric accuracy. If the signal increases to a value that was 25% greater than its initial value the interferogram is rejected.
- A periodic interference caused by wind-induced vibrations is usually of too low frequency to cause a problem. In any event, the effect of this interference is eliminated by a high-pass filter, implying that the use of additional instrument and reflector enclosures would be beneficial.
- The noise level of the interferogram (and hence of the spectrum) sometimes increased dramatically because of the effect of electrical interference. To allow excessively noisy interferograms to be recognized, the noise level index given in Eq. (2) is calculated after the high-pass filter has been applied to the target interferogram.
- Broad spikes were sometimes observed in the interferogram because of the passage of objects (e.g., birds or vehicles) through the beam; these spikes rarely presented a problem and their effect was usually removed by the high-pass filter. The effect of a single narrow spike could not be readily recognized but when narrow spikes were observed, they always occurred in groups. In this case, they had the same effect as high-frequency noise and the affected interferograms could be rejected using the same criterion.

Table 1
Summary of the percentage of scans taken during long periods of data acquisition during March and June 2005, and January 2006 that were rejected using the criteria described in this paper

Time	Rejected/total	Percentage rejected (%)
March 21–22	0/919	0.0
March 20–21	13/1608	0.8
March 19–20	6/1116	0.5
March 18–19	0/1184	0.0
March 17–18	0/1222	0.0
March 16–17	108/1213	8.9
March 15–16	46/1195	3.8
June 27–28	4/1192	0.3
June 26–27	50/1238	4.1
June 25–26	111/1108	10
June 24–25	12/1234	1.0
June 23–24	0/1145	0.0
January 31–February 1	576/1190	48
January 28–29	280/1131	25
January 27–28	0/1177	0.0
January 25–26	0/976	0.0
January 24–25	249/1356	18

Using the above five criteria, a procedure was developed to automatically scrutinize each interferogram immediately after it was measured. By this procedure, most invalid interferograms were identified and rejected automatically. Table 1 shows the number of interferograms that were rejected for representative ~24-h periods of data acquisition. On calm summer (and even some winter) days, no interferograms were rejected. Conversely, almost half of the interferograms were automatically rejected on one particularly windy winter day using the criteria described in this paper. We would note that our measurements were made at a nominal resolution of 1 cm^{-1} by averaging 16 forward and 16 reverse interferograms, even though only the forward scan was used for the data analysis. If lower resolution can be tolerated, the number of interferograms averaged in a given time can be further increased, yet it will not completely eliminate the effects of these interferences. No matter how many scans are averaged, however, a QA/QC procedure analogous to the one outlined above should be implemented.

Acknowledgments

This work was funded under Cooperative Agreement 58-5368-3-269 with the United States Department of Agriculture, Agricultural Research Service, Northwest Irrigation and Soils Research Laboratory, Kimberly, Idaho. We would also like to thank Norimasa Iwata and Brandy Eastman for assistance in acquiring the data.

References

[1] G.M. Russwurm, J.W. Childers, Open-path Fourier transform infrared spectroscopy, in: J.M. Chalmers, P.R. Griffiths (Eds.), Handbook of Vibrational Spectroscopy, vol. 2, Wiley, New York, 2002.

[2] A.R. Newman, Anal. Chem. 69 (1) (1997) 43A–47A.

[3] W.T. Walter, in: Proceedings of SPIE—The International Society for Optical Engineering, vol. 5270 (Environmental Monitoring and Remediation III), 2004, pp. 144–150.

[4] J.W. Childers, E.L. Thompson, D.B. Harris, D.A. Kirchgessner, M. Clayton, D.F. Natschke, W.J. Phillips, Atmos. Environ. 35 (11) (2001) 1923–1936.

[5] G.M. Russwurm, Long-path open-path Fourier transform infrared monitoring of atmospheric gases: compendium method TO-16, in: Compendium of Methods for the Determination of Toxic Organic Compounds in Ambient Air, 2nd ed., Center for Environmental Research Information, Office of Research and Development, US Environmental Protection Agency, Cincinnati, OH, 1997 (EPA/625/R-96/010b).

[6] Standard guide for open-path Fourier transform infrared (OP/FTIR) monitoring of gases and vapors in air, E-1865-97, in: Annual Book of ASTM Standards, American Society for Testing and Materials, vol. 03.06, West Conshohocken, PA, 1997.

[7] Standard practice for open-path Fourier transform infrared (OP/FTIR) monitoring of gases and vapors in air, E-1982-98, in: Annual Book of ASTM Standards, American Society of Tests and Materials, West Conshohocken, vol. 03.06, PA, 1998.

[8] B.K. Hart, R.J. Berry, P.R. Griffiths, Environ. Sci. Technol. 34 (2000) 1346.

[9] B.K. Hart, P.R. Griffiths, in: Proceedings of 11th International Conference on Fourier Transform Spectroscopy, Am. Inst. Phys. Conf. Proc. 430 (1998) 241.

[10] D.B. Chase, Appl. Spectrosc. 38 (1984) 491.

[11] P.R. Griffiths, J.A. de Haseth, Fourier Transform Infrared Spectrometry, Wiley-Interscience, New York, 1986, pp. 74–76.

[12] P.R. Griffiths, J.A. de Haseth, Fourier Transform Infrared Spectrometry, Wiley-Interscience, New York, 1986, pp. 267–268.